Excitation of cavitation bubbles in low-temperature liquid nitrogen

Koichi Sasaki* and Shingo Harada

Division of Quantum Science and Engineering, Hokkaido University, Sapporo 060-8628, Japan

We excited a cavitation bubble by irradiating a Nd:YAG laser pulse onto a titanium target that was installed in liquid nitrogen at a temperature below the boiling point. To our knowledge, this is the first experiment in which a cavitation bubble has been successfully excited in liquid nitrogen. We compared the cavitation bubble in liquid nitrogen with that in water on the basis of an equation reported by Florschuetz and Chao [J. Heat Transfer **87**, 209 (1965)].

Liquid-phase laser ablation attracts considerable attention as a new method for synthesizing functional nanomaterials.[1,2] This method has an advantage in the use of no chemicals. Crystalline nanoparticles with unique structures are synthesized,[3–7] which is another advantage of liquid-phase laser ablation. A mechanism for the synthesis of crystalline nanoparticles is considered to be related to the high pressure of the plasma produced by laser irradiation in a liquid environment.[8] In addition, the role of a cavitation bubble in the synthesis of nanoparticles has been pointed out recently. It has been shown that the reaction field for the growth of nanoparticles is the inside of the cavitation bubble.[9–12] Since the cavitation bubble at its collapse has a high pressure,[13] the structure of synthesized nanoparticles is affected by the dynamics of the cavitation bubble.[14,15]

The medium used most widely in liquid-phase laser ablation is water. Nanoparticles of noble metals and oxidized materials are synthesized by laser ablation in water. On the other hand, approximately ten years ago, we tried laser ablation in liquid nitrogen as a method for synthesizing nitride nanoparticles.[16] However, the cavitation bubble was not excited in liquid nitrogen at 77 K in atmospheric pressure.[17,18] Therefore, we could not utilize the high pressure of the collapsed cavitation bubble in the synthesis of nitride nanoparticles by laser ablation in liquid nitrogen. In this work, we demonstrated the excitation of cavitation bubbles in liquid nitrogen by reducing its temperature below the boiling point. To our knowledge, this is the first experiment in which cavitation bubbles have been excited in liquid nitrogen.

The experimental apparatus used is schematically shown in Fig. 1. We prepared a coaxial

*E-mail address: sasaki@qe.eng.hokudai.ac.jp

cylindrical chamber composed of four shells to realize laser ablation in liquid nitrogen at various temperatures. The four shells had quartz windows. The outermost shell (shell 1 in Fig. 1) was evacuated using a turbomolecular pump for thermal isolation. The second shell (shell 2) was filled with liquid nitrogen. Although liquid nitrogen in shell 2 was always at the boiling point, it was possible to control the temperature below 77 K by reducing its pressure using an oil rotary pump. The third shell (shell 3) was also filled with liquid nitrogen. The pressure in shell 3 was controlled between 0.1 and 0.2 MPa. The liquid nitrogen in shell 3 was cooled down by thermal conduction from shell 2 to obtain liquid nitrogen at a temperature lower than the boiling point. The innermost shell (shell 4) was a small cylinder for collecting nanoparticles after the experiment. Liquid nitrogen in shell 4 had the same temperature and the same pressure as those in shell 3.

A titanium target was installed on a rotatable holder in shell 4. We used a Nd:YAG laser at a wavelength of 532 nm to ablate the titanium target. The energy and duration of the Nd:YAG laser pulse were 60 mJ and 8 ns, respectively. A lens was placed in shell 2 to focus the laser beam onto the target. The region in front of the target was observed by shadowgraph imaging. The light source was a metal halide lamp, and the pattern of the transmitted lamp light was captured using a high-speed camera with a flame rate of 200 kHz. The high-speed camera was replaced by a charge-coupled device camera with a gated image intensifier (ICCD camera) when we needed a higher temporal resolution. The temperature of liquid nitrogen was monitored by measuring the electric resistance of a platinum wire.

Figure 2 shows the shadowgraph images observed when the pressure and temperature of liquid nitrogen in shell 4 were 0.1 MPa and 77 K, respectively. The images were extracted from the high-speed movie. The times indicated below the images are the delay times after the irradiation of the Nd:YAG laser pulse. As shown in Figs. 2(a)-2(c), we observed the formation and expansion of a bubble from the irradiation point of the Nd:YAG laser pulse. After the maximum size was observed at $\sim$ 170 μs after the laser irradiation, we observed the change in bubble shape from hemispherical to distorted, as shown in Figs. 2(d)-2(f). After that, we observed that the bubble was shredded into small bubbles, as shown in Figs. 2(g)-2(i). The shrinkage of the bubble was never observed when the pressure and temperature were 0.1 MPa and 77 K, respectively. In contrast, we observed the shrinkage of the bubble when we cooled the liquid nitrogen below the boiling point. Figure 3 shows the shadowgraph images observed when the pressure and temperature of liquid nitrogen in shell 4 were 0.1 MPa and 66 K, respectively. After the maximum size was observed at $\sim$ 155 μs after the laser irradiation [Fig. 3(c)], we observed the shrinkage of the bubble as shown in Figs. 3(d)-

3(f). The shrinkage was followed by the collapse and reformation of the secondary bubble, as shown in Figs. 3(g)-3(i). The maximum size of the secondary bubble was smaller than that of the first bubble.

The temporal variations of the bubble sizes, which were observed under three experimental conditions, are plotted in Fig. 4. Although the shape of the bubble induced at a temperature of 77 K and a pressure of 0.1 MPa was not hemispherical after the maximum size, the distance between the target surface and the leading edge of the bubble is plotted in Fig. 4. The shrinkage, collapse, and rebound of the bubble were clearly observed when the temperature of liquid nitrogen was 66 K. Note here that the secondary bubble had a similar lifetime to the first bubble in spite of its smaller size when the pressure was 0.1 MPa. When we pressurized the liquid nitrogen in shell 4 up to 0.2 MPa, we observed a smaller bubble with a shorter lifetime, as shown in Fig. 3. In this case, we observed the formation of the third cavitation bubble after the collapse of the second bubble.

The bubble radii plotted in Fig. 4 were obtained from movies captured using a high-speed camera. Since the temporal resolution of the high-speed camera (5 μs) was insufficient to capture the collapsed bubble, we examined the the size of the bubble at its collapse using an ICCD camera with a gate width of 50 ns. As a result, the radius of the collapsed cavitation bubble, which was induced at a pressure of 0.2 MPa and a temperature of 66 K, was identified to be 0.16 mm. A shockwave was not generated at the collapse of the bubble, even though the gate width of 50 ns was sufficient to capture the wavefront of the shockwave with a propagation speed of approximately 1100 m/s.

Florschuetz and Chao have reported that the bubble dynamics is understood on the basis of the parameter defined by[19)]

$$B_{\mathrm{eff}} = \psi^2 \left[\frac{\rho c(T_{\mathrm{b}} - T_\infty)}{\bar{\rho}_{\mathrm{v}} L}\right]^2 \frac{\kappa}{R_0}\left(\frac{\rho}{p_\infty - p_{\mathrm{v}0}}\right)^{1/2}, \tag{1}$$

where ρ, c, κ, and T_{b} are the density, specific heat, thermal diffusivity, and boiling point of the liquid, respectively, L is the latent heat, R_0 is the maximum bubble radius, T_∞ is the temperature of the liquid at a long distance from the bubble, and $p_{\mathrm{v}0}$ and p_∞ are the vapor pressures at T_∞ and T_{b}, respectively. ψ is called the temperature difference correction factor, which is given by

$$\psi = \frac{2}{(T_{\mathrm{b}} - T_\infty)(p_\infty - p_{\mathrm{v}0})} \int_{T_\infty}^{T_{\mathrm{b}}} [p_\infty - p_{\mathrm{v}}(T)]\mathrm{d}T, \tag{2}$$

where $p_{\mathrm{v}}(T)$ represents the temperature dependence of the vapor pressure, and $\bar{\rho}_{\mathrm{v}}$ is the aver-

age vapor density defined by

$$\bar{\rho}_{\mathrm{v}} = \frac{1}{T_{\mathrm{b}} - T_{\infty}} \int_{T_{\infty}}^{T_{\mathrm{b}}} \rho_{\mathrm{v}}(T)\mathrm{d}T, \tag{3}$$

where $\rho_{\mathrm{v}}(T)$ represents the temperature dependence of the equilibrium vapor density. According to Florschuetz and Chao, the bubble dynamics is dominated by the liquid inertia when $B_{\mathrm{eff}} \geq 10$, and in this case, the hard collapse of the bubble is realized. On the other hand, when $B_{\mathrm{eff}} \leq 0.05$, the heat transfer controls the bubble dynamics, and in this case, the shrinkage and collapse of the bubble become weaker.

Table I shows the B_{eff} values obtained under the experimental conditions in Fig. 4. B_{eff} under a typical experimental condition of laser ablation in water is also shown in Table I for comparison. We ignored the temperature dependences of the thermodynamic parameters in the evaluation of B_{eff}. As shown in Table I, $B_{\mathrm{eff}} \geq 10$ is realized in water, such that we observe the hard collapse of the cavitation bubble with the generation of a shockwave in laser ablation in water.[20] The experimental result shown in Fig. 2 is understood reasonably by considering $B_{\mathrm{eff}} = 0$ in liquid nitrogen at 77 K (boiling point).

B_{eff} in liquid nitrogen is much smaller than that in water even when the temperature was reduced below the boiling point. The reasons for the small B_{eff} in liquid nitrogen are the small temperature difference from the boiling point and the large equilibrium vapor density. The maximum B_{eff} we realized in this experiment was 1.2×10^{-2}. The heat transfer controls the bubble dynamics under the present experimental conditions according to Florschuetz and Chao, but we realized the bubbles with the dynamics of shrinkage, collapse, and rebound. Because of these dynamics, we may categorize the bubble as "a cavitation bubble". However, the dynamics of the cavitation bubbles in liquid nitrogen was less energetic than that in water. The less energetic dynamics is understood by the large radius of the collapsed bubble (0.16 mm in liquid nitrogen and 0.07 mm in water[20]), the negligible generation of the shockwave, and the long lifetime of the secondary bubble at a temperature of 66 K and a pressure of 0.1 MPa.

In conclusion, we have succeeded in the excitation of a cavitation bubble with the dynamics of shrinkage, collapse, and rebound in liquid nitrogen by reducing its temperature below the boiling point. To our knowledge, this is the first experiment in which a cavitation bubble has been successfully excited in liquid nitrogen. However, the dynamics of the cavitation bubble in liquid nitrogen was less energetic than that in water, which is understood by fact that B_{eff} in liquid nitrogen is much smaller than that in water.

References

1) F. Mafuné, J. Kohno, Y. Takeda, T. Kondow, and H. Sawabe, J. Phys. Chem. B **104**, 8333 (2000).
2) F. Mafuné, J. Kohno, Y. Takeda, T. Kondow, and H. Sawabe, J. Phys. Chem. B **104**, 9111 (2000).
3) G. W. Yang, J. B. Wang, and Q. X. Liu, J. Phys.: Condens. Matter **10**, 7923 (1998).
4) P. Liu, Y. L. Cao, H. Cui, X. Y. Chen, and G. W. Yang, Chem. Mater. **20**, 494 (2008).
5) X. Y. Chen, H. Cui, P. Liu, and G. W. Yang, Chem. Mater. **20**, 2035 (2008).
6) C. H. Liang, Y. Shimizu, T. Sasaki, and N. Koshizaki, Appl. Phys. A **80**, 819 (2005).
7) D. Amans, A.-C. Chenus, G. Ledoux, C. Dujardin, C. Reynaud, O. Sublemontier, K. Masenelli-Varlot, and O. Guillois, Diamond Relat. Mater. **18**, 177 (2009).
8) H. Ushida, N. Takada, and K. Sasaki, J. Phys.: Conf. Ser. **59**, 563 (2007).
9) W. Soliman, N. Takada, and K. Sasaki, Appl. Phys. Express **3**, 035201 (2010).
10) S. Ibrahimkutty, P. Wagener, A. Menzel, A. Plech, and S. Barcikowski, Appl. Phys. Lett. **101**, 103014 (2012).
11) S. Ibrahimkutty, P. Wagener, T. S. Rolo, D. Karpov, A. Menzel, T. Baumbach, S. Barcikowski, and A. Plech, Sci. Rep. **5**, 16313 (2015).
12) M. Takeuchi and K. Sasaki, Appl. Phys. A **122**, 312 (2016).
13) C. Brennen, *Cavitation and Bubble Dynamics* (Oxford University Press, Oxford, U.K., 1995).
14) W. Soliman, N. Takada, N. Koshizaki, and K. Sasaki, Appl. Phys. A **110**, 779 (2013).
15) N. Takada, Fujikawa, N. Koshizaki, and K. Sasaki, Appl. Phys. A **110**, 835 (2013).
16) N. Takada, T. Sasaki, and K. Sasaki, Appl. Phys. A **93**, 833 (2008).
17) N. Takada, T. Nakano, and K. Sasaki, Appl. Phys. A **101**, 255 (2010).
18) H. Sato, X. W. Sun, M. Odagawa, K. Maeno, and H. Honma, J. Fluids Eng. **118**, 850 (1996).
19) L. W. Florschuetz and B. T. Chao, J. Heat Transfer **87**, 209 (1965).
20) K. Sasaki, T. Nakano, W. Soliman, and N. Takada, Appl. Phys. Express **2**, 046501 (2009).

Figure captions

Fig. 1. (Color online) Schematic of the experimental apparatus.

Fig. 2. Shadowgraph images observed at various delay times after the irradiation of the Nd:YAG laser pulse: (a) 0 μs, (b) 5 μs, (c) 125 μs, (d) 325 μs, (e) 400 μs, (f) 3.8 ms, (g) 5.7 ms, (h) 13 ms, and (i) 19 ms. The pressure and temperature of liquid nitrogen were 0.1 MPa and 77 K, respectively.

Fig. 3. Shadowgraph images observed at various delay times after the irradiation of the Nd:YAG laser pulse: (a) 0 μs, (b) 45 μs, (c) 155 μs, (d) 250 μs, (e) 275 μs, (f) 300 μs, (g) 440 μs, (h) 580 μs, and (i) 640 μs. The pressure and temperature of liquid nitrogen were 0.1 MPa and 66 K, respectively.

Fig. 4. (Color online) Temporal variation in bubble radius after the irradiation of the Nd:YAG laser pulse.

Table I. Evaluation of B_{eff} given by Eq. (1) under the present experimental conditions. B_{eff} under a typical condition of laser ablation in water is also shown for comparison.

Medium	p_∞ (MPa)	T_∞ (K)	$T_\mathrm{b} - T_\infty$ (K)	$\bar{\rho}_\mathrm{v}$ (kg/m^3)	R_0 (mm)	B_{eff}
Liquid N_2	0.1	77	0	4.4	1.5	0
Liquid N_2	0.1	66	11	2.4	1.8	0.9×10^{-2}
Liquid N_2	0.2	66	18	3.6	1.3	1.2×10^{-2}
Water	0.1	300	73	0.2	1	13

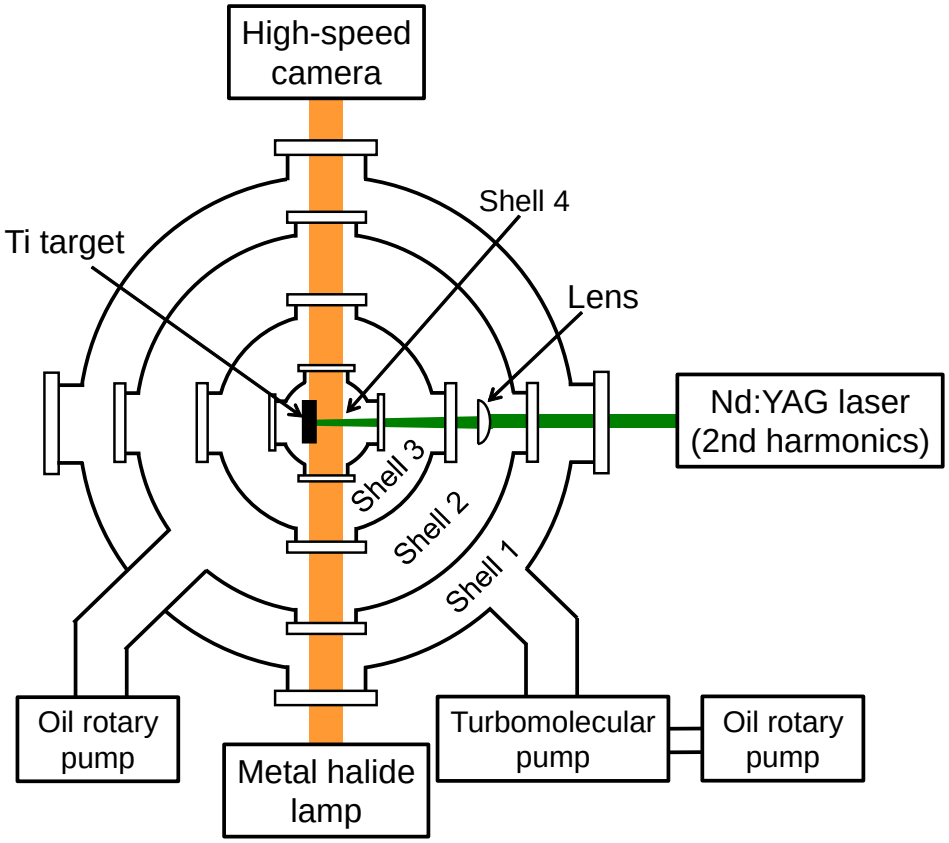

Fig. 1. (Color online) Schematic of the experimental apparatus.

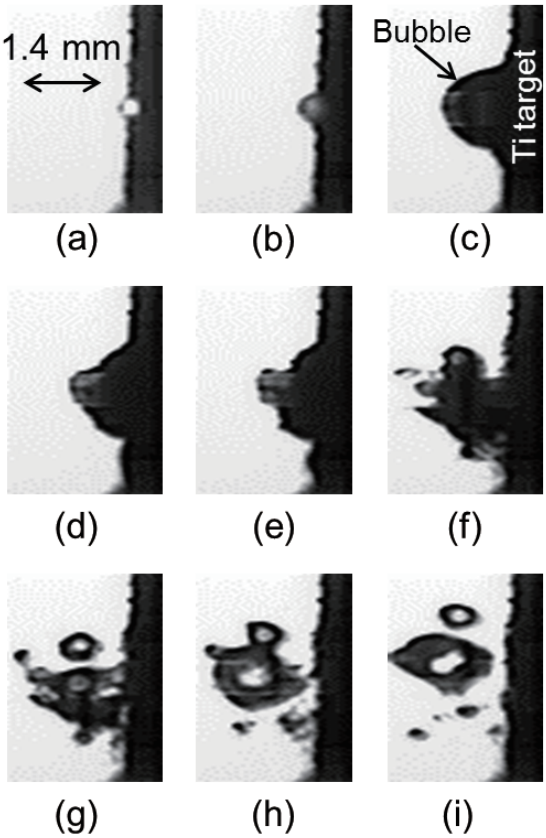

Fig. 2. Shadowgraph images observed at various delay times after the irradiation of the Nd:YAG laser pulse: (a) 0 μs, (b) 5 μs, (c) 125 μs, (d) 325 μs, (e) 400 μs, (f) 3.8 ms, (g) 5.7 ms, (h) 13 ms, and (i) 19 ms. The pressure and temperature of liquid nitrogen were 0.1 MPa and 77 K, respectively.

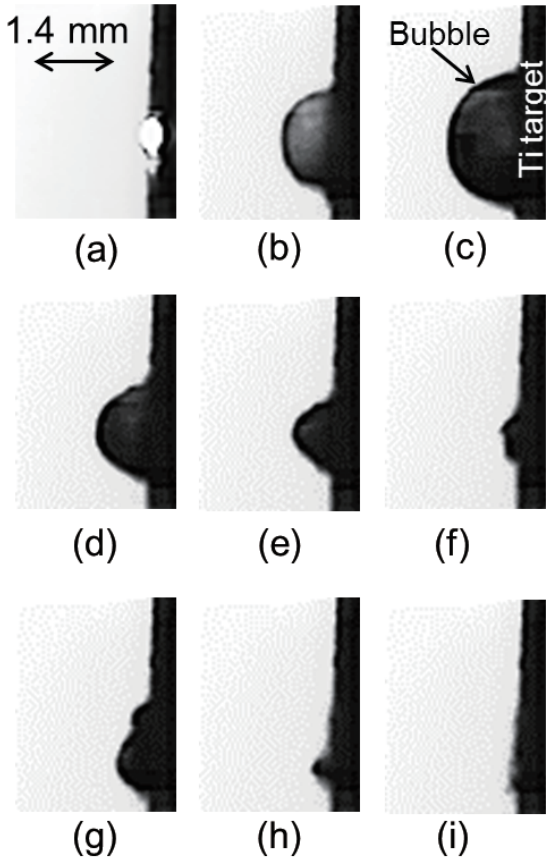

Fig. 3. Shadowgraph images observed at various delay times after the irradiation of the Nd:YAG laser pulse: (a) 0 μs, (b) 45 μs, (c) 155 μs, (d) 250 μs, (e) 275 μs, (f) 300 μs, (g) 440 μs, (h) 580 μs, and (i) 640 μs. The pressure and temperature of liquid nitrogen were 0.1 MPa and 66 K, respectively.

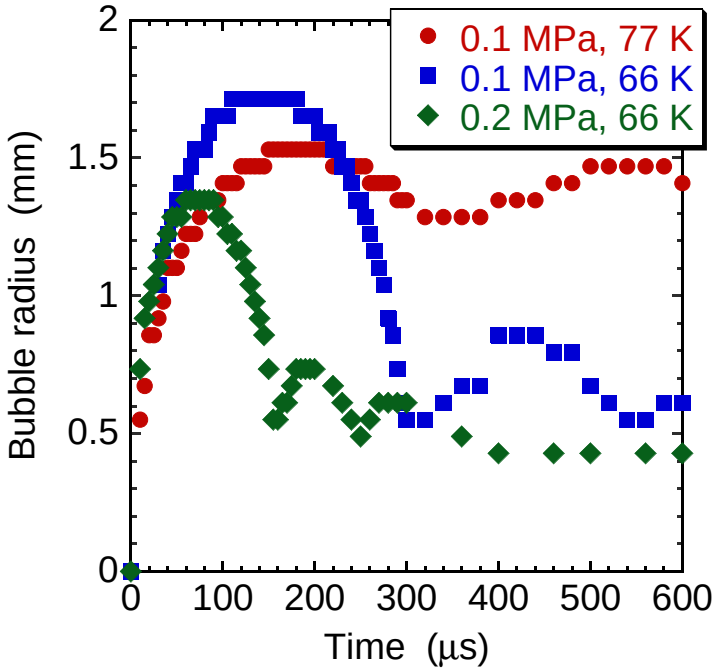

Fig. 4. (Color online) Temporal variation in bubble radius after the irradiation of the Nd:YAG laser pulse.